Available online at www.sciencedirect.com
ScienceDirect
Catalysis Today 133–135 (2008) 99–105
CATALYSIS TODAY
www.elsevier.com/locate/cattod

Preparation and characterization of bifunctional catalysts of the Pd, Pt/H[Ga]MFI types

Luis Melo [a,b,*], Yraida Díaz [b], Marta Mediavilla [a], Aura Llanos [b,c], Alberto Albornoz [b], Joaquín L. Brito [b,**]

[a] *Facultad de Ingeniería, Universidad Central de Venezuela (UCV), P.O. Box 48.057, Caracas 1041-A, Venezuela*
[b] *Laboratorio de Fisicoquímica de Superficies, Centro de Química, Instituto Venezolano de Investigaciones Científicas (IVIC), P.O. Box 20632, Caracas 1020-A, Venezuela*
[c] *Departamento de Química, Instituto Universitario de Tecnología-Región Capital (IUT-RC), Caracas, Venezuela*

Available online 12 February 2008

Abstract

An MFI type galosilicate was synthesized and characterized employing XRD, N_2 adsorption at −196 °C, chemical analysis by ICP-AES, and XPS. This material was used in the preparation of Pd/H[Ga]ZSM5 and Pt/H[Ga]ZSM5 bifunctional catalysts, calcined under dry air for 6 h at 500 and 300 °C, respectively, and then reduced "in situ" under H_2 flow for 6 h at 500 °C. The bifunctional catalysts were also characterized by XRD, N_2 physisorption, TEM, chemical analysis, and XPS. The support possesses an MFI structure with excellent crystallinity, as shown by XRD. Bulk chemical analysis shows a $(Si/Ga)_{ICP\text{-}AES}$ atomic ratio of 16. The absence of Ga_2O_3 is suggested by both XRD and XPS (at surface level). The atomic ratio at the surface, $(Si/Ga)_{XPS}$, is the same as that found by ICP-AES, suggesting that Ga is distributed homogeneously. XRD and N_2 physisorption results of the bifunctional catalysts suggest that metal incorporation does not affect sensibly the structure of the support. Dispersion of Pd and Pt in either catalyst was estimated from TEM analysis, indicating in both cases values of the order of 80%. The atomic ratios $(Si/Ga)_{XPS}$ at the surface were 16 for Pd/Galosilicate, and 4 for Pt/Galosilicate, suggesting that Pt promotes migration of Ga towards the external surface of the solid, a phenomenon that is not observed for the Pd/H[Ga]ZSM5 catalyst. Degaliation promoted by Pt could be explained assuming that Pt and Ga could form stable chemical species, as might be indicated by XPS results. The transformation of acetone to MIBK was employed as catalytic test. These results indicate very different behaviors for either bifunctional catalyst.

Keywords: Bifunctional catalysts; Pd, Pt/H[Ga]MFI; XPS; TEM; XRD characterization; Migration of Ga

1. Introduction

Supported metal catalysts have been in the forefront of heterogeneous catalysts for many years. These catalysts are widely used since they combine the desirable catalytic properties of the metal with the enhanced activity resulting from being dispersed on a high surface area material. Interest in gallium-containing MFI-type zeolites stems from their high selectivity to aromatics in the catalytic conversion of olefins and paraffins, the so-called Cyclar process [1], and also from their high catalytic activity for vapour phase conversion of phenol and ammonia mixtures into aniline [2]. Gallium species are said to be effective in various forms: incorporated into the zeolitic framework, impregnated [3], ion exchanged [4], or even as physical mixtures of H-ZSM5 and Ga_2O_3 [5]. For gallosilicates, which could contain two types of gallium species, the catalytic roles of framework and extra-framework gallium has been a matter of interest. Although it is not accurately known how these catalysts work, the studies of characterization carried out on these solids have allowed to determine that species such as Ga_2O_3, generated in the surface of these solids, are seemingly reduced to Ga^+ ions [6]. These species have also been found in systems that consist of physical mixtures of Ga_2O_3 and protonic zeolites, as well as in zeolites exchanged with aqueous solutions of Ga^{3+} precursors. It has also been detected that gallium migrates from the surface (*i.e.*,

* Corresponding author at: Facultad de Ingeniería, Universidad Central de Venezuela (UCV), P.O. Box 48.057, Caracas 1041-A, Venezuela.
Tel.: +58 212 6053091; fax: +58 212 6053034.
** Corresponding author.
E-mail addresses: melol@ucv.ve (L. Melo), joabrito@ivic.ve (J.L. Brito).

0920-5861/$ – see front matter © 2007 Elsevier B.V. All rights reserved.
doi:10.1016/j.cattod.2007.12.113

impregnated or ion exchanged species) toward the framework; this phenomenon has been attributed to the mobility of gallium under the action of thermal treatments [7]. On the other hand, in solids with structural gallium, the migration of Ga^{3+} has been observed from the framework positions toward the surface, with formation of Ga_2O_3 that then could transform in other species such as Ga_2O, Ga^+, Ga^0 [8].

Supports of the H[Ga]MFI family are being employed with increasing frequency in the preparation of bifunctional catalysts of the metal/H[Ga]MFI type, because the resulting solids generally show a high dispersion of the supported metal phase, as well as an appropriate strength and density of acid sites to catalyze chemical reactions of industrial interest. In this sense, in the scientific literature a large number of works employing this type of catalysts can be found for applications in petrochemical processes [9–13] and fine chemical synthesis [14,15]. One reason for this is that these solids are very active, selective and stable in reactions such as hydro-dehydrogenation and isomerization [11,16,17]. Recently, however, results that throw some doubts on the potential of Pt/H[Ga]ZSM5 catalysts for hydrogenation reactions have been reported [7,18,19], showing a relatively low activity of these solids, that has been assigned to a passivation of the metallic centers probably originated in an interaction of the supported phase with extra-structural Ga species (Ga_2O_3, Ga_2O, Ga^+, Ga, *etc.*), which migrate or are formed on the surface of the galosilicate [19].

The purpose of the present work is to contribute to the study of the passivation problem of the Pt metallic centers by gallium, comparing the Pt systems with the analog Pd/H[Ga]ZSM5 catalysts, employing a series of characterization techniques, such as XRD, ICP-AES elemental analysis, N_2 physisorption, TEM and XPS. To further characterize both sets of catalysts, the transformation of acetone to methyl-isobutyl-ketone, MIBK, under standard conditions [14,20] is employed as test reaction. This reaction is well suited to evaluate bifunctional catalysts, such as those reported in the present work, as it requires both acidic (for aldolization and dehydration steps) and metallic functions (selective hydrogenation of an α,β-unsaturated ketone; for a detailed reaction scheme, see below).

2. Experimental

An MFI-type galosilicate was synthesized by the method of Guth and Caullet [21]. After washing and drying it was calcined in dry air at 550 °C. The solid obtained was exchanged with a 2 M $NH_4C_2H_3O_2$ solution, dried and calcined again at 550 °C under dry air, allowing to obtain the protonic form, H[Ga]ZSM5. Thereafter, this galosilicate was characterized by powder X-ray diffraction (XRD, Siemens D-5005 instrument, employing Cu Kα radiation) to check its crystalline structure; N_2 physisorption at −196 °C (Micromeritics 2010 instrument) to measure BET specific surface area (ASS), chemical analysis by inductively coupled plasma-atomic emission spectroscopy (ICP-AES, EAA-LL CGB, PerkinElmer), allowing to verify the bulk atomic ratio $(Si/Ga)_{ICP\text{-}AES}$, and finally, X-ray photoelectron spectroscopy (XPS, ESCALAB 220i-XL spectrometer, VG Scientific), in order to determine surface chemical species as well as the surface atomic ratio $(Si/Ga)_{XPS}$. The solid thus obtained and characterized was employed as support in the preparation of two bifunctional catalysts: 1 wt%Pd/H[Ga]ZSM5 and 1 wt%Pt/H[Ga]ZSM5, by means of the exchange–impregnation method [18], using as metal precursors $Pd(NH_3)_4Cl_2$ and $Pt(NH_3)_4Cl_2$ (both from Aldrich). The resulting impregnated solids were first dried and then calcined for 6 h under dry air flow at 500 (Pd) and 300 °C (Pt). Afterwards, they were reduced "in situ" under H_2 flow for 6 h at 500 °C. The resulting bifunctional catalysts (Pd/H[Ga]ZSM5 and Pt/H[Ga]ZSM5) were evaluated by powder XRD, to check if the introduction of metals affect the crystallinity of the support; ICP-AES to measure the actual metal content; transmission electron microscopy (TEM, Hitachi CM-10 equipment operated at 120 kV), to determine the dispersion, *D*, of the metallic phase on the galosilicate surface; BET surface area by physisorption of N_2; and XPS, to check the state of surface species in the catalysts surfaces. Samples for TEM, XPS and activity measurements were reduced "in situ" under flowing H_2 at 500 °C. The catalysts were evaluated using as test reaction the transformation of acetone at 160 °C, 1 atm total pressure, acetone/H_2 atomic ratio = 3, and variable WHSV. Analysis of the reactor effluent was carried out by means of a HP-6890 gas chromatograph with FID detector and a CP-Sil 5CB column of 30 m length and 0.25 mm diameter. This analytical methodology presents a relative error that does not exceed 2%.

3. Results and discussion

3.1. Catalysts characterization

Evaluation by XRD of the support shows that it possesses an MFI type structure with high purity and crystallinity, as can be appreciated in Fig. 1a. The same technique indicated that for both bifunctional catalysts the introduction of the metals does not bring about noticeable structural changes in the support, as can be seen for the 1 wt%Pd/H[Ga]ZSM5 catalyst (Fig. 1b).

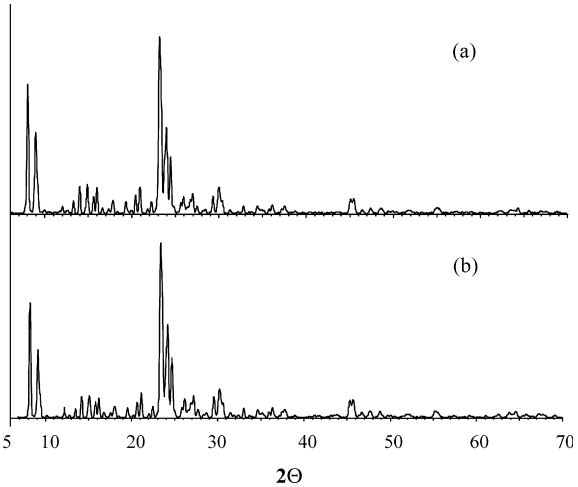

Fig. 1. Powder X-ray diffractograms of: (a) H[Ga]ZSM5 and (b) 1 wt%Pd/H[Ga]ZSM5.

Table 1
Physicochemical characteristics of the support and the supported catalysts

Catalysts	$(Si/Ga)_{ICP}$	$(Si/Ga)_{XPS}$	M (wt%)[a]	SSA (m^2/g)	$D\ (\%)_{TEM}$
H[Ga]ZSM5	16	15	–	380	–
1.00%Pd/H[Ga]ZSM5	16	16	1.02	375	77
1.00%Pt/H[Ga]ZSM5	16	4	0.98	370	84

[a] M = Pd or Pt.

Specific surface areas (SSA) of both support and catalysts measured by N_2 physisorption (BET method) showed values between $370 - 380\ m^2/g$, as shown in Table 1. These are typical values for this type of material, suggesting that neither the support nor the catalysts present blockage for the access of N_2 molecules to the inner porous structure.

In Table 1 it can also be appreciated that the $(Si/Ga)_{ICP\text{-}AES}$ bulk atomic ratios for the catalysts are similar to that of the support. Thus, again, the introduction of metals seems not to affect the physicochemical characteristics of the support [18]. Metal (Pd and Pt) contents were also determined by ICP-AES and it can be seen that the real contents are very close to the nominal (1 wt%), showing that the impregnation–exchange procedure is appropriate to synthesize this kind of solids.

3.2. Transmission electron microscopy analysis

If we accept that hydrogenation reactions of unsaturated multiple C=C bonds depend on the nature of the metallic phase as well as on the number of accessible metallic centers for the reactants, it is essential then to define the phase to be supported (in the present case Pd and Pt) and to determine the population of metallic centers scattered on the surface of the support employed. This evaluation was carried out by means of TEM, a technique that allows to estimate the mean diameter of the metallic particles present in the catalysts. Fig. 2a and b show typical micrographs for either bifunctional catalyst (1 wt%Pd/H[Ga]ZSM5 and 1 wt%Pt/H[Ga]ZSM5, respectively). The statistical analysis normally employed to obtain the dispersion of the supported metallic phase starts by counting the frequency of apparition of particles of a given size (di, diameter in nm), which results in the histograms shown in Fig. 2c and d. The number of particles counted for each micrograph was of the order of 500, and several micrographs per sample were analyzed. From this data, the mean diameter of the particles [d (nm)], can be obtained from the expression: $d = \Sigma nidi^3/\Sigma nidi^2$ [22]. With the mean diameter of particles, the dispersion of the metals can be calculated employing the equation proposed by Boudart [23]: $D(\%) \cong 100/d$ (nm), which is a good approximation for transition metals. The results obtained suggest that the mean diameters of Pd and Pt particles are close to 1.2 nm, meaning that the dispersions of the metallic phases are of the order of 80% in both cases.

3.3. X-ray photoelectron spectroscopy analysis

In order to establish which are the chemical species present in the surfaces of the catalysts, XPS was carried out in the C 1s, O 2s, Si 2p, Ga 3d, Pd 3d, and Pt 4f regions. The different signals were referred to the C 1s one at 284.6 eV [24].

In Fig. 3 the XPS signals in the Ga 3d region are shown for the following solids: Ga_2O_3 (employed as standard); H[Ga]ZSM5; 1 wt%Pd/H[Ga]ZSM5; and 1 wt%Pt/H[Ga]ZSM5, all after calcination and reduction (c,r). Fig. 3a, for Ga_2O_3 (c,r) shows

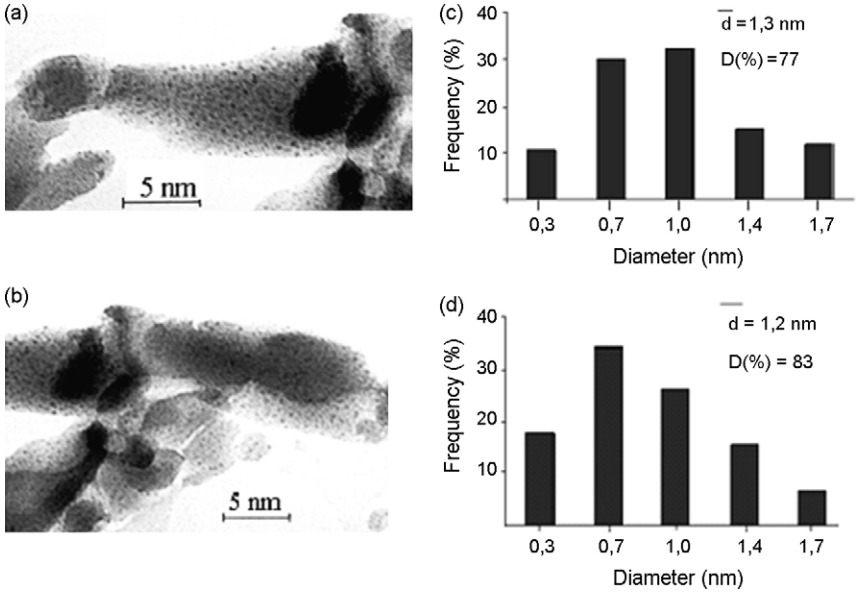

Fig. 2. TEM micrographs for the catalysts: (a) 1 wt%Pd/H[Ga]ZSM5; (b) 1 wt%Pt/H[Ga]ZSM5; (c) distribution of particle sizes of 1 wt%Pd/H[Ga]ZSM5; (d) distribution of particle sizes of 1 wt%Pt/H[Ga]ZSM5.

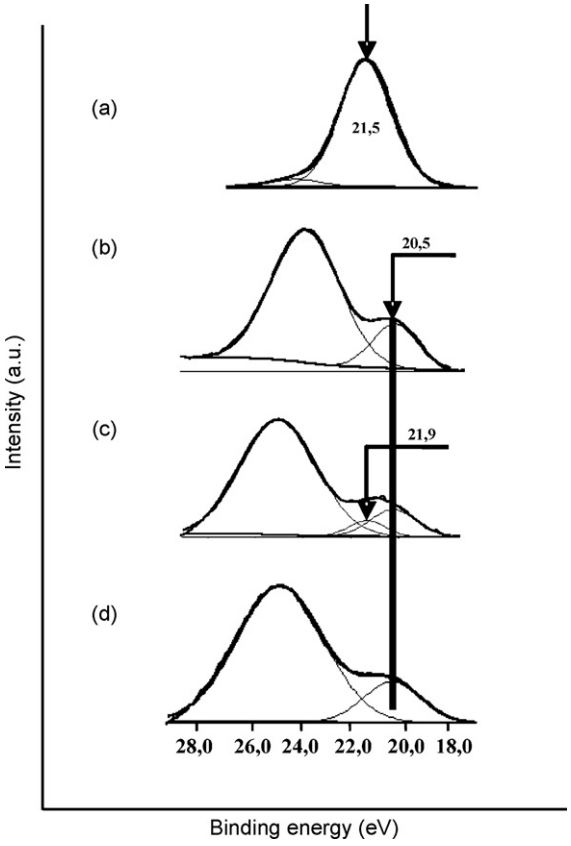

Fig. 3. X-ray photoelectron spectra in the Ga 3d region for: (a) Ga_2O_3 (c,r); (b) H[Ga]ZSM5 (c,r); (c) 1 wt%Pt/H[Ga]ZSM5(c,r); (d) 1 wt%Pd/H[Ga]ZSM5 (c,r).

an intense signal at 21.5 eV. Considering that in this oxide Ga coordination is mostly octahedric [25], this peak is assigned to Ga(III)[O].

On the other hand, in Fig. 3b corresponding to H[Ga]ZSM5 (c,r), it can be appreciated a single signal centered at 20.5 eV, which can be assigned to tetrahedrally coordinated Ga, *i.e.*, Ga(III)[T]. This assignation is based on the fact that in this material Ga has been incorporated not by impregnation or exchange but by incorporation in the synthesis gel, thus minimizing the possibility of segregation to extra-structural positions, as shown by the XRD results in Fig. 1a. Our results disagree with those reported by Nowak et al. [26], who found extra-structural Ga_2O_3 species, although their synthesis method was rather different from ours.

Fig. 3c show the Ga 3d XPS spectrum for the 1 wt%Pt/H[Ga]ZSM5(c,r) catalyst. After curve-fitting (''deconvolution'') two peaks at 20.5 and 21.9 eV can be appreciated. According to the assignations for 3a and 3b, the first signal corresponds to Ga(III)[T], and the second one to Ga(III)[O]. Thus, the latter peak would likely be due to extra-framework Ga species. Elsewhere it was reported that the size of this peak seems to increase with increasing Pt content in the catalyst [18]. For 1 wt%Pd/H[Ga]ZSM5(c,r) (Fig. 3d), a single signal with a binding energy (BE) of 20.5 eV was observed, in agreement with the sole presence of Ga(III)[T] species, as in the case of the support. Thus, Pd behaves distinctly from Pt, and does not promote the migration of Ga species from the MFI network to extra-structural surface positions, a phenomenon that, indeed, is observed in the Pt/H[Ga]ZSM5 solid (Fig. 3c). These results seem to confirm that incorporation of Pt to galosilicates stimulates Ga migration from framework to extra-framework positions, a process that could be driven by the formation of stable surface Pt-Ga species, *e.g.*, alloys, as suggested by Chao et al. [7] and Cao and Jiang [19]. More recently, Mikhailov et al. [27], by means of simulation through the GAMESS US program package, foresee the presence of a Ga_2Pt_4 cluster located into the channels of the Pt/H[Ga]ZSM5 solid. Another possibility is the formation at the surface of Pt–Ga mixed oxides [18], also leading to passivation of surface Pt species.

Characterization by XPS allows to evaluate how the deposition of the metals could affect the composition of the surface of the catalysts. In this sense, the $(Si/Ga)_{XPS}$ atomic ratio calculated from the intensity of the Si 2p and Ga 3d peaks is shown in Table 1. For both the support and the Pd/H[Ga]ZSM5 catalyst it was found a similar value of 16 as that determined by ICP-AES for the same samples. For the Pt/H[Ga]ZSM5 sample, on the other hand, $(Si/Ga)_{XPS}$ shows a lower value of 4 than that obtained from the bulk ICP-AES analysis (Table 1). This, again, is consistent with migration of Ga to the surface of the catalysts, most likely promoted by Pt.

Analysis of the Pd/H[Ga]ZSM5(c) (only calcined) and Pd/H[Ga]ZSM5(c,r) (calcined and reduced) samples by XPS in the Pd 3d region is shown in Fig. 4. The spectrum of the calcined sample was curve-fitted using three signals with BE of 336.5, 337.2, and 338.2 eV (Pd $3d_{5/2}$ signal); these were assigned to $Pd–O_{ads}$, PdO and Pd^+ species [28], respectively. After reduction, the curve-fitting procedure resulted in a decreased number of signals, with BE of 334.9 and 336.0 eV, which were assigned [29] to Pd^0 aggregates, and Pd^0 atomically dispersed, respectively. Thus, for the present Pd catalysts the reduction pretreatment has an important effect on the state of the metal, as

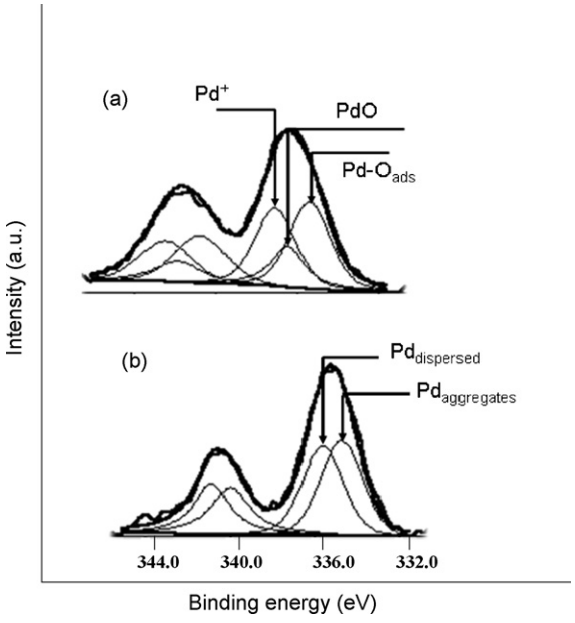

Fig. 4. X-ray photoelectron spectra in the Pd 3d region for: (a) 1 wt%Pd/H[Ga]ZSM5(c) and (b) 1 wt%Pd/H[Ga]ZSM5(c,r).

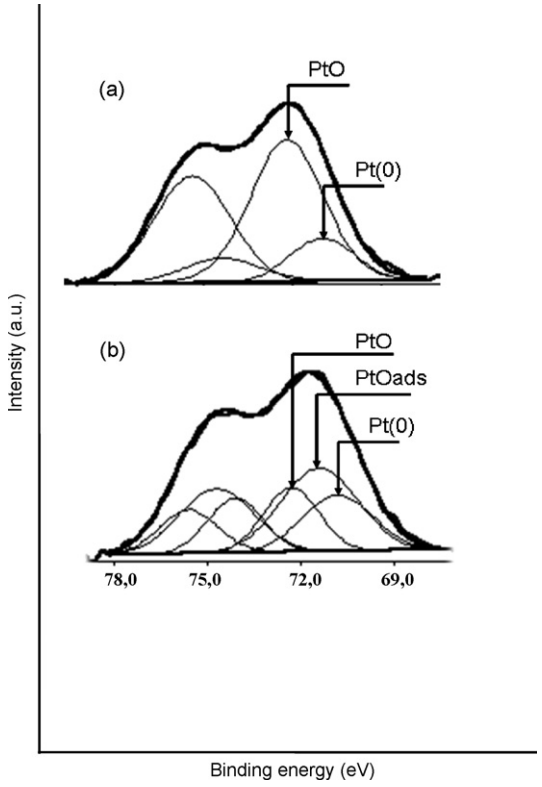

Fig. 5. X-ray photoelectron spectra in the Pt 4f region for: (a) 1%wtPt/H[Ga]ZSM5(c) and (b) 1%wtPt/H[Ga]ZSM5(c,r).

all Pd oxidic species present in the calcined precursor are reduced fully to the metallic state, which does not happen in the case of the Pt catalysts (see below).

Finally, the XP-spectra in the Pt 4f region for Pt/H[Ga]ZSM5 samples, both calcined (c) and calcined and reduced (c,r) are shown in Fig. 5. In the spectrum of the calcined sample, Fig. 5a, shows two peaks at BE of 72.8 and 71.6 eV (Pt $4f_{7/2}$ peak). Normally, Pt signals at BE values below 71.8 eV are assigned to metallic Pt [24,30], thus the peak at 71.6 eV could be related to well dispersed Pt^0 nanoparticles interacting with the zeolitic support to which it could transfer electronic density, thus forming $Pt^{+\delta}$ species. The signal at 72.8 eV might be assigned to PtO; however, this BE is significantly lower than that normally related to Pt(II) oxidic species, around 73.3 eV [24]. Interestingly, this signal seems to be exclusive of the Pt/[Ga]ZSM5 solid, as it was not found in the case of a Pt/[Al]ZSM5 sample [18]. A possibility is that the lower BE reflects the interaction of the surface Pt(II) species

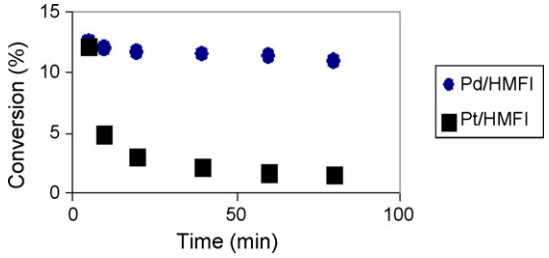

Fig. 6. Evolution the acetone conversion as function of the reaction time at 160 °C, 1 atm, PAc/P H_2 = 3 and WHSV = 9.4 h^{-1}.

with the Ga(III)[O] (Ga_2O_3) extra-framework ones, possibly with formation of mixed Pt–Ga oxides.

Fig. 5b shows the XP-spectrum in the Pt 4f region for the (c,r) sample. In this case, three signals had to be used to curve-fit the experimental spectrum, with BE of 72.8, 71.6, and 70.8 eV. It can be easily seen that reduction of the bifunctional Pt/H[Ga]ZSM5 catalyst results in a strong diminution of the peak at 72.8 eV and corresponding increase of the other two peaks. Thus, Pt(II) species, most likely interacting with the Ga(III)[O] ones, would be redispersed upon reduction, forming nanoparticles (see TEM results) of metallic Pt (peak at 71.6 eV) which interact with the support forming small electrodeficient clusters, $Pt^{+\delta}$ and/or a complex species such as Pt-O_{ads}, explaining the transfer of electronic density to the support. This type of reduced Pt species were already present in the calcined state of the catalyst (Fig. 5a). Another kind of Pt metallic species is found that gives rise to the signal at a BE of 70.8 eV, associated to Pt^0 [24,31], most likely aggregates of larger size than those related to the 71.6 eV peak. As the concentration of Pt species is proportional to the area of the different signals, most of the Pt present in the reduced catalyst corresponds to species with BE of 72.8 and 71.6 eV, *i.e.*, Pt(II) plus $Pt^{+\delta}$ interacting with Ga_2O_3 and/or Pt-O_{ads}. In either case, these are species that should increase the energy of adsorption of hydrogen [32], thus they would be less active in hydrogenation processes.

3.4. Catalytic evaluation

The support, as well as the bifunctional catalysts synthesized and characterized as described above, were employed in the transformation of acetone to MIBK, in the conditions described in Section 2. Acetone transformation occurs according to the following reaction scheme:

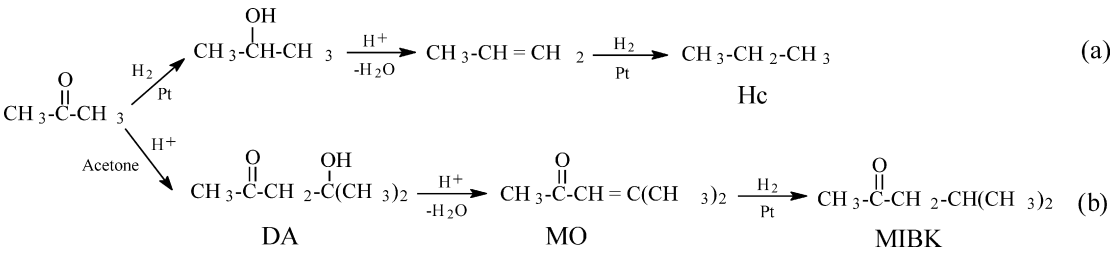

(1)

Reaction branch (a): Hydrogenation of the carbonylinic double bond of the propanone, forming isopropanol, which by acid catalysis dehydrates to propene; this alkene is then hydrogenated to produce propane [14].

Reaction branch (b): Aldolization of two acetone molecules via acid catalysis to produce first the intermediate diacetone alcohol (DA), which then dehydrates to mesitil oxide (MO), again by acid catalysis and probably on the same sites where DA was produced; selective hydrogenation of the olefinic bond of MO renders the asymmetric ketone, MIBK [14,20].

As can be seen, the desired transformation, branch (b), requires well balanced acid and hydro/dehydrogenating functions in the catalysts and thus is well suited to test bifunctional catalysts as those synthesized in the present work.

Effluents of the reactor were analyzed, and the following components were identified and quantified: methyl-isobutyl-ketone (MIBK); propane (Hc); mesityl oxide (MO); 2-methyl pentane (2MP); and a trace of di-isobutyl-ketone (DIBK). Fig. 6 presents the evolution of conversion in function of time for Pd/H[Ga]ZSM5 and Pt/H[Ga]ZSM5 catalysts at a WHSV of 9.4 h^{-1}. It can be appreciated that both catalysts possess similar initial activities; however, the Pd/Galosilicate catalyst shows a good stability, which is not observed for the Pt catalyst. That difference must be the reflection of the varying physicochemical characteristics of the catalysts. As can be seen in Table 1, both solids show practically the same dispersion of the supported phase and both show quite the same density of acid sites, thus, similar catalytic properties in the transformation of acetone to MIBK could be expected, specially considering that both Pd and Pt catalysts should be able to hydrogenate C=O and C=C bonds involved in this chemical transformation. Now, it is known that in a typical hydrogenation transformation, *i.e.*, benzene hydrogenation, the following order of reactivity for transition metals of the group 10 has been reported: Pt > Ni > Pd [33]. Thus, a higher activity would be anticipated for Pt/H[Ga]ZSM5 as compared with Pd/H[Ga]ZSM5, contrary to what is observed experimentally. In Table 2 the selectivity towards the different products at 10% isoconversion of acetone is shown. The Pd/Galosilicate catalyst produces three times more MIBK than the Pt/Galosilicate one; also, the Pt catalyst produces 65 times more MO than the Pd-based solid. This, of course, indicates that the metallic centers of platinum are poorly active for the hydrogenation of MO to MIBK, thus this intermediate accumulates in the Pt system. While several similarities between these solids are evident (see, *e.g.*, Table 1) it must be noted that XPS analysis demonstrates that in the Pt/Galosilicate catalyst a large fraction of platinum is in oxidic form, both as Pt(II) plus $Pt^{+\delta}$ interacting with Ga_2O_3 and/or Pt-O_{ads} (Pt $4f_{7/2}$ peaks at 72.8 and 71.6 eV). These types of species should not be very active for hydrogenation reactions [32], and would not contribute to the acetone transformation to MIBK. On the other hand, the Pd/Galosilicate solids seems to be a more equilibrated catalyst: as shown by XPS, most of the supported phase is Pd^0, which must have a high selectivity for hydrogenation of the olefinic (C=C) bond respect the carbonylic (C=O) one, given by the low adsorption of carbonylic groups on Pd particles. This is attributed to the change of electronic structure in atoms of Pd (change from the $4d^{9.7}5s^{0.3}$ configuration to the $4d^{10}5s^0$ one) provoked by the hydrogen atoms absorbed in the metal particles [34]. This change in electronic configuration would induce a selective adsorption of MO trough the C=C functionality, which would be selectively (90%) hydrogenated to MIBK on the Pd/Galosilicate.

Table 2
Selectivity at 10% conversion in the acetone transformation for 1 wt%Pd/H[Ga]ZSM5 and 1 wt%Pt/H[Ga]ZSM5

Products	1 wt%Pd/H-[Ga]ZSM5	1 wt%Pt/H-[Ga]ZSM5
Hc	4	7
2MP	2	0
MIBK	91	28
MO	1	65
DIBK	2	0

4. Conclusions

Palladium/Galosilicate catalysts, contrary to the Platinum/Galosilicate ones, are able to hydrogenate preferentially the olefinic unsaturation of the mesityl oxide intermediate, thus the products of reaction on the Pd system are rich in MIBK (90% selectivity). This may be due to the fact that supported Pd is well dispersed and forming mostly Pd^0 particles, which adsorb selectively the olefinic double bond of MO. Regarding the Pt/Galosilicate catalyst, platinum seems to stimulate migration of Ga from framework to extra-framework positions, forming Ga_2O_3 which seems to interact with the Pt particles rendering them inactive for hydrogenation reactions. This could be the result either of interaction Pt–Ga, forming mixed oxides, or Ga inducing a redispersion of Pt, leading to too small clusters in close interaction with the support. The ($Pt^{+\delta}$) and/or Pt-O_{ads} thus formed would have a low activity for hydrogenation processes.

Acknowledgements

The authors would like to acknowledge the technical help of Mr. J.L. Prins, IIBCA-UDO, in the acquisition of the TEM micrographs. Special thanks to FONACIT, Project QF-10, and the Laboratorio Nacional de Química Analítica for the use of the XPS instrument.

References

[1] J.R. Mowry, R.F. Anderson, J.A. Jhonson, Oil Gas J. (1985) 128.
[2] N. Katada, S. Kuroda, M. Niwa, Appl. Catal. A: Gen. 180 (1999) 1.
[3] C.R. Bayense, A.J.H.P. van der Pol, J.H.C. van Hoof, Appl. Catal. 72 (1991) 153.
[4] N.S. Gnep, J.Y. Doyemet, M. Guisnet, Stud. Surf. Sci. Catal. 46 (1989) 153.
[5] V.I. Yakerson, T.V. Vasina, L.I. Lafer, V.P. Sytnyk, G.L. Dylch, A.V. Mokhov, O.V. Bragin, Kh.M. Minachev, Catal. Lett. 3 (1989) 339.
[6] G.L. Price, V. Kanazirev, J. Catal. 126 (1990) 267.
[7] K.J. Chao, A. Wu, J.F. Lee, Micropor. Mesopor. Mater. 35/36 (2000) 443.
[8] K. Nishi, S.I. Komai, K. Inagaki, A. Satsuma, T. Hattori, Appl. Catal. A: Gen. 223 (2002) 187.

[9] V.R. Choudhary, A.K. Kinage, T.V. Choudhary, Appl. Catal. A: Gen. 162 (1997) 239.
[10] J.A. Rabo, Zeolite Chemistry and Catalysis, ACS Monograph 171 American Chemical Society, Washington, 1976.
[11] M. Guisnet, G. Perot, in: F.R. Ribeiro, et al. (Eds.), Zeolite: Science and Technology, NATO ASI, 80, Martinus Nijhoff Publishers, The Hague, 1984, p. 397.
[12] P. Mériaudeau, C. Naccache, J. Mol. Catal., A: Chem. 59 (1990) L31–L36.
[13] M. Guisnet, N.S. Gnep, F. Alirio, Appl. Catal., A: Gen. 89 (1992) 1.
[14] L. Melo, P. Magnoux, G. Giannetto, F. Alvarez, M. Guisnet, J. Mol. Catal., A: Chem. 124 (1997) 155.
[15] N. Lavuad, P. Magnoux, F. Alvarez, L. Melo, G. Giannetto, M. Guisnet, J. Mol. Catal., A: Chem. 142 (1999) 223.
[16] Ch. Kappenstain, M. Guerin, K. Lázar, K. Matussek, Z. Paál, J. Chem. Soc., Faraday Trans. 94 (1998) 2463.
[17] A. Corma, A. Martínez, in: E.G. Derouane, et al. (Eds.), Catalytic Activation and Functionalisation of Light Alkanes: Advances and Chalenges, Kluwer Academic Publishers, 1998, p. 35.
[18] Y. Díaz, L. Melo, M. Mediavilla, A. Albornoz, J.L. Brito, J. Mol. Catal., A: Chem. 227 (2005) 7.
[19] Y.C. Cao, X.Z. Jiang, J. Mol. Catal., A: Chem. 242 (2005) 119.
[20] L. Melo, A. Llanos, L. García, P. Magnoux, F. Alvarez, M. Guisnet, G. Giannetto, Catal. Lett. 51 (1998) 207.
[21] J.L. Guth, Ph. Caullet, J. Chim. Phys. 83 (1986) 155.
[22] T.E. Whyte Jr., Catal. Rev. -Sci. Eng. 8 (1973) 117.
[23] M. Boudart, H.S. Hwang, J. Catal. 39 (1975) 44.
[24] K.S. Kim, N. Winograd, R.E. Davis, J. Am. Chem. Soc. 93 (1971) 6296.
[25] I.A. Sheka, I.S. Chaus, T.T. Mityureva, The Chemistry of Gallium, Elsevier Publishing Co., Amsterdam, 1966, p. 32.
[26] I. Nowak, J. Quartararo, E.G. Derouane, J.C. Védrine, Appl. Catal. A: Gen. 251 (2003) 107.
[27] M.N. Mikhailov, I.V. Mishin, L.M. Kustov, A.L. Lapidus, Micropor. Mesop. Mater. 104 (2007) 145.
[28] M. Bancroff, I. Adams, L. Coatsworth, D. Bennewitz, J. Brown, W. Westwood, Anal. Chem. 47 (1975) 586.
[29] A. Reddy, M.A. Genhaw, J. Bockris, J. Chem. Phys. 48 (1968) 671.
[30] P. Mériaudeau, C. Naccache, A. Thangaraj, C.L. Bianchi, R. Carli, S. Narayanan, J. Catal. 152 (1995) 313.
[31] D. Brigg, M.P. Seah (Eds.), Practical Surface Analysis by Auger and X-ray Photoelectron Spectroscopy, Wiley, New York, 1983.
[32] W.M.H. Sachtler, A.Y. Stakheev, Catal. Today 12 (1992) 283.
[33] J.F. Le Page, J. Cosyns, P. Courty, E. Freund, J.P. Franck, Y. Jacquin, B. Jugun, C. Marcilly, G. Martino, J. Miguel, R. Montarnal, A. Sugier, H. Van Landeghan, Catalyse de contact, conception, preparation et mise en ouvre des catalyseurs industriels, Ed. Technip, Paris, 1967, p. 365.
[34] V. Ponec, Appl. Catal., A: Gen. 149 (1997) 27.